J Clust Sci (2017) 28:393–411
DOI 10.1007/s10876-016-1107-7

ORIGINAL PAPER

Nanofabrication of Graphene Quantum Dots with High Toxicity Against Malaria Mosquitoes, *Plasmodium falciparum* and MCF-7 Cancer Cells: Impact on Predation of Non-target Tadpoles, Odonate Nymphs and Mosquito Fishes

Kadarkarai Murugan[1,2] · Devaraj Nataraj[3] · Anitha Jaganathan[1] · Devakumar Dinesh[1] · Sudalaimani Jayashanthini[1] · Christina Mary Samidoss[1] · Manickam Paulpandi[1] · Chellasamy Panneerselvam[1,4] · Jayapal Subramaniam[1,5] · Al Thabiani Aziz[4] · Marcello Nicoletti[6] · Suresh Kumar[7] · Akon Higuchi[8] · Giovanni Benelli[9]

Received: 5 October 2016 / Published online: 21 October 2016

Abstract Recently, it has been highlighted an overlooked connection between the biting activity of *Anopheles* mosquitoes and the spread of cancer. The excellent physico-chemical properties of graphene quantum dots (GQDs) make them a suitable candidate for biomedical applications. We focused on the toxicity of GQDs

✉ Giovanni Benelli
benelli.giovanni@gmail.com

[1] Division of Entomology, Department of Zoology, School of Life Sciences, Bharathiar University, Coimbatore, Tamil Nadu 641046, India

[2] Department of Zoology, Thiruvalluvar University, Serkkadu, Vellore, Tamil Nadu 632115, India

[3] Department of Physics, Bharathiar University, Coimbatore, Tamil Nadu 641046, India

[4] Department of Biology, Faculty of Science, University of Tabuk, Tabuk 71491, Saudi Arabia

[5] Division of Vector Biology, Department of Zoology, Faculty of Science, Annamalai University, Annamalai Nagar, Cuddalore, Tamil Nadu 608 002, India

[6] Department of Environmental Biology, Sapienza University of Rome, Piazzale Aldo Moro 5, 00185 Rome, Italy

[7] Department of Medical Microbiology and Parasitology, Universiti Putra Malaysia (UPM), Serdang, Malaysia

[8] Department of Chemical and Materials Engineering, National Central University, No. 300 Jhongli, Taoyuan 32001, Taiwan

[9] Department of Agriculture, Food and Environment, University of Pisa, Via del Borghetto 80, 56124 Pisa, Italy

against *Plasmodium falciparum* and its vector *Anopheles stephensi,* and their impact on predation of non-target mosquito predators. Biophysical methods, including UV–vis, photoluminescence, FTIR and Raman spectroscopy, XRD analysis and TEM, confirmed the effective GQD nanosynthesis. LC_{50} against *A. stephensi* ranged from 0.157 (larva I) to 6.323 ppm (pupa). The antiplasmodial activity of GQDs was evaluated against CQ-resistant (CQ-r) and CQ-sensitive (CQ-s) strains of *P. falciparum*. IC_{50} were 82.43 (CQ-s) and 85.17 μg/ml (CQ-r). In vivo experiments conducted on *Plasmodium berghei* infecting albino mice showed moderate activity of GQDs if compared to chloroquine. Concerning non-target effects, the predation efficiency of *Gambusia affinis*, *Anax immaculifrons* and *Hoplobatrachus tigerinus* post-treatment with GQDs was enhanced. Lastly, GQDs were toxic against MCF-7 breast cancer cell lines with an $IC_{50} = 24.81$ μg/ml, triggering apoptosis in treated cells. Overall, we highlighted the multipurpose potential of GQDs for the development of newer drugs in the fight against *Anopheles* vectors, *Plasmodium* parasites and breast cancer cells.

Keywords *Anopheles stephensi* · Biosafety · Nanoparticles · Non-target effects

Introduction

Graphene quantum dots (GQDs) recently emerged as superior and universal fluorophores, due to their unique combination of a number of key merits, including excellent photo-stability, small size, biocompatibility, highly tunable photoluminescence (PL), exceptional multi-photon excitation (up-conversion), electrochemiluminescence, chemical inertness, and simple functionalization routes with biomolecules [1]. For these reasons, GQD synthesized by various top-down and bottom-up approaches [2] are presently at the center of research efforts to develop low-toxicity, environmentally friendly alternatives to conventional semiconductor quantum dots [3, 4].

Because of their small size and biocompatibility, they may also serve as effective carriers for drug delivery, allowing simultaneous visual monitoring of releasing kinetics [5]. GQDs can be also useful in chemotherapeutics for the treatment of cancer as well as for the differentiation and imaging of stem cells [6]. Moreover, GQDs functionalized with various functional groups (e.g. NH_2, COOH, and CO–N $(CH_3)_2$) showed cytotoxicity towards A549 cells [7]. However, it should be mentioned that most of the existing cytotoxicity studies are based on MTT assay, and a systematical cytotoxicity evaluation is necessary for the biocompatibility assessment of GQDs [8].

Interestingly, GQDs have been also proposed as possible candidates to develop newer and safer larvicides in mosquito control programs [9, 10], even if field evidences on a wider scale are lacking [11]. Mosquitoes (Diptera: Culicidae) act as vectors for a number of important pathogens and parasites, including malaria, avian malaria, yellow fever, dengue, chikungunya, Zika virus, Rift valley fever, Japanese encephalitis, Western equine encephalomyelitis, bancroftian and brugian filariae, canine heartworm disease (*Dirofilaria immitis*) and setariosis (*Setaria* spp.) [11–16].

Anopheles stephensi is vector of *Plasmodium* parasites (Protozoa) responsible for causing malaria. There were about 198 million cases of malaria in 2013 and an estimated 584,000 deaths. However, malaria mortality rates have fallen by 47 % globally since 2000 and by 54 % in the African region. Most deaths occur among children living in Africa, where a child dies every minute from malaria. Malaria mortality rates among children in Africa have been reduced by an estimated 58 % since 2000 [17]. However, the resurgence of malaria after eradication in many countries is still documented [18, 19]. The clinical manifestations of malaria are due to the invasion and destruction of red blood cells by the parasite and the consequent host reaction to the malarial parasite infection [20]. However, the extent of hemolysis in malaria is much greater than that seen in other parasite-induced hemolysis pathways [21]. In addition, it has been recently pointed out an overlooked connection between the biting activity of *Anopheles* mosquitoes and the spread of cancer, with special reference to USA [22, 23], and several relevant analogies at the physiological level among cancer pathology and mosquito-borne diseases have been also outlined [24], highlighting the urgent need of effective multipurpose drugs for joint treatment of cancer and mosquito-borne diseases (see [25] for a recent review).

The better strategy to lower the incidence of mosquito-transmitted diseases and to avoid further complications is to avoid mosquito bites using adult repellents as well as microbial and chemical pesticides. Mosquito young instars have less mobility in their breeding habitat, thus control measures at this stage are relative easy [26]. In their early days of use, chemical pesticides (e.g. carbamates, organophosphates and pyrethroids) showed success in reducing vector populations. However, their frequent overuse increased selection pressure on mosquitoes creating resistance to commonly used molecules [27–29]. Moreover, chemical insecticides also lead to important concerns for the environment and human health [13, 30, 31]. Therefore, in the latest years, a number of eco-friendly mosquito control tools have been proposed [13]. Recently, a number of plant extracts and related metabolites have been exploited for efficient and rapid extracellular synthesis of mosquitocidal nanocomposites with high effectiveness, even if field conditions (e.g. [11, 15, 32–37]).

However, most of the researches focused on the one-pot and cheap nanosynthesis of metal nanoparticles (see [25] for a recent review), while carbon ones have been scarcely studied [9, 10]. Starting from the connection between *Anopheles* biting activity and the spread of cancer in USA [24], in this research we focused on the toxicity of nanofabricated GQDs against human breast cancer cells (MCF-7 strain), chloroquine-resistant (CQ-r) and CQ-sensitive (CQ-s) strains of *Plasmodium falciparum* and young instars of its mosquito vector *A. stephensi.* The antiplasmodial activity of GQDs was also studied through in vivo experiments on *P. berghei* infecting albino mice. As regards to non-target effects, the predation efficiency of mosquito natural enemies i.e. *Gambusia affinis* adults, *Anax immaculifrons* nymphs and *Hoplobatrachus tigerinus* tadpoles, post-treatment with ultra-low doses of GQDs was evaluated. In addition, a wide array of biophysical methods, including UV–vis, photoluminescence, FTIR and Raman spectroscopy, XRD analysis and TEM, was employed to confirm the effective and cheap nanosynthesis of GQDs.

Materials and Methods

Chemicals

Graphite, HCl, H_2SO_4, $KMnO_4$, H_2O_2, FeSo4, Giemsa stain, PBS, sodium chloride, EDTA, Tris, DMSO and Triton X-100, NaOH, Tris buffer, sodium hypochlorite, saponin and SYBR Green were all of analytical grades and were purchased from Sigma Aldrich (USA). Fetal bovine serum, penicillin, streptomycin were purchased from Himedia (India). Throughout the study, double distilled water, milli-Q grade water was used for all the experiments, with the exception of mosquito assays, for which dechlorinated water was employed.

Nanosynthesis and Characterization of Graphene Quantum Dots

Graphene oxide was prepared following the modified method by Hummers [38]. 1.0 g of graphite and 60 mL H_2SO_4 (98 %) was stirred in an ice bath, and 5.8 g $KMnO_4$ was slowly added with stirring for 0.5 h. The solution was heated to 30 °C for 2 h, 40 mL of deionizer water was added slowly, the reaction was heated to 90 °C for 30 min, then 80 mL of deionizer water was added. When the temperature was cooled down to 60 °C, 10 mL H_2O_2 (30 %) were added to obtain an orange yellow solution. 200 mL of 5 % HCl solution was added, the supernatant was decanted and centrifuged with deionizer water to pH 4–6, and the mixture solution was further dialyzed in a dialysis bag for 2 days. Low density graphene oxide was obtained by lyophilizing at −48 °C, 21 Pa, and GO was obtained as gray-yellow powder.

To fabricate GQDs, we followed the method by Murugan et al. [10]. We suspended grapheme oxide (1.0 g) in concentrated H_2SO_4 for a period of 1–2 h in an ice-water bath and then treated them with 50 % (wt) $KMnO_4$. The H_2SO_4 conditions aid in shearing the graphene oxide. The reaction mixture was stirred at room temperature for 2 h and then heated to 45–50 °C for additional 1 h. Distilled water (40 mL) was slowly dropped into the resulting solution. Finally, the reaction temperature was rapidly increased to 90 °C with effervescence for 30 min. When all the $KMnO_4$ was consumed, we quenched the reaction by pouring over ice containing a small amount of H_2O_2 followed by distilled water (70 mL) obtaining a yellow transparent solution instantly. After cooling down to room temperature, the mixture was ultra-sonicated mildly for a few minutes, the pH was tuned to 8.0 by NaOH in an ice bath, and we found a black flocculent deposit. Then, the pH was increased to 4.0 adding HCl. The suspension was filtered through a 0.22 μm microporous membrane to remove the large tracts of graphene oxide, and deep yellow solution (yield ca. 36 %) was separated. The mixture solution was further dialyzed in a dialysis bag (retained molecular weight: 3,000 to 8,000 Da), and greenish fluorescent GQDs were obtained (yield ca. 34.8 %).

GQDs were characterized using including UV–vis, photoluminescence, FTIR and Raman spectroscopy and XRD analysis [10]. Size analysis of colloidal GQDs was carried out using TEM-JEM-2100F at a voltage of 200 kV. The samples were

prepared by mounting a drop of the aqueous suspension containing the GQDs on a carbon grid, which then was placed on filter paper to absorb excess solvent. The average particle diameter and size distribution were calculated using Java Image tool software, based on the data of an average of 70–100 particles.

Cytotoxicity on Breast Cancer Cells

Human breast cancer cell line (MCF-7 strain) was purchased from National Centre for Cell Sciences (NCCS, Pune, India). The cells were maintained in DMEM with 10 % fetal bovine serum, 1 % penicillin and 0.5 % streptomycin. The cultured cells were cultured at 37 °C in a 5 % CO_2 humidified incubator.

Cell proliferation was monitored by 3-(4,5-dimethylthiazol-2-yl)- 2,5-di-phenyl-tetrazolium bromide (MTT) assay, as described by Mosmann [39], with slight modification by Murugan et al. [40]. Exponentially growing MCF 7 cells (1×10^4 cells per mL) were seeded in 96-well plates in a final volume of 100 mL per well and treated with series (1–50 mg ml^{-1}) of test samples (GQDs) in FCS free complete medium for 48 h. 100 mL of MTT (5 mg ml^{-1}) were added to treated cells, and the plates were incubated at 37 °C for 4 h. The supernatant was aspirated and 100 mL of DMSO was added to each well to dissolve the formosan crystals. Absorbance was measured at 620 nm using a 96-well microplate reader (Lambda 1050 Perkin Elmer) and the inhibitory concentration (IC_{50}) was was calculated. The percentage of cell survival was calculated using the following formula: [41]:

$$\text{Relative cell survival } (\%) = (\text{mean experimental cell absorbance } (\text{A620})/ \text{mean control cell absorbance } (\text{A620})) \times 100$$

Flow cytometry was used to detect apoptotic cells with diminished DNA content [42]. MCF-7 cells were seeded into 6-well plates at 1×10^5 cells/well. Post-treatment with GQDs, the cells were fixed in ice-cold 70 % ethanol at −20 °C overnight. After centrifugation and washing one time with PBS, low-molecular-weight DNA was extracted using 0.2 mol/L phosphate–citrate buffer and stained with 200 µL of 1 mg/mL propidium iodine (PI)/10 mL, and 0.1 % Triton X-100/ 2 mg DNase-free RNase A. The solution was incubated for 30 min at room temperature in the dark, followed by flow cytometric analysis at 488 nm (BD, Franklin Lakes, NJ, USA).

Hemolysis on Red Blood Cells

Hemolysis activity was evaluated on the blood of one healthy donor (from Bharathiar University, Coimbatore, India). 5 mL of whole blood sample was added to 10 mL of Ca- and Mg-free Dulbecco's phosphate buffered saline (Sigma-Aldrich, USA) and centrifuged at 500 g for 10 min to isolate red blood cells (RBCs) from the serum. This purification was repeated five times, and then the washed RBCs were diluted to 50 mL in PBS. 1, 5, 10, 15, 20, 25 µL of grapheme oxide suspended in tyrode, tyrode (negative control) or triton X-100 (positive control) were added to 5 µL of washed RBC suspension. The suspension was incubated at room temperature

on a shaking plate for 1, 4 and 24 h. After the incubation time, the suspension was centrifuged at 10000g over 5 min. Supernatant was read on a 96-well plate using a microplate scanning spectrophotometer XMark (Lambda 1050 Perkin Elmer) at 550 nm. The hemolysis (%) was calculated as:

$$\mathrm{H}\ (\%) = (\mathrm{OD550nm\ sample} - \mathrm{OD550nm\ tyrode})/(\mathrm{OD550nm\ Triton\ X} - 1001\% - \mathrm{OD550nm\ tyrode}) \times 100$$

Anopheles stephensi Rearing

Following the method by Murugan et al. [43], eggs of *A. stephensi* were provided by the National Centre for Disease Control (NCDC) field station of Mettupalayam (Tamil Nadu, India). For both species, eggs were transferred to laboratory conditions [27 ± 2 °C, 75–85 % R.H., 14:10 (L:D) photoperiod] and placed in 18 × 13 × 4 cm plastic containers containing 500 mL of tap water, waiting for larval hatching [44, 45]. Larvae were reared in the containers and fed daily with a mixture of crushed dog biscuits (Pedigree, USA) and hydrolyzed yeast (Sigma-Aldrich, Germany) at a 3:1 ratio (w:w). Water was renewed every two days. The breeding medium was checked daily and dead individuals were removed. Breeding containers were kept closed with muslin cloth to prevent contamination by foreign mosquitoes. Pupae were collected daily from culture containers and transferred to glass beakers containing 500 mL of water. Each glass beaker contained about 50 mosquito pupae and was placed in a mosquito-rearing cage (90 × 90 × 90 cm, plastic frames with chiffon walls) until adult emergence. Mosquito adults were continuously provided with 10 % (w:v) glucose solution on cotton wicks. The cotton was always kept moist with the solution and changed daily. Five days after emergence, females were supplied with a blood meal which was furnished by means of professional heating blood (lamb blood), at a fixed temperature of 38 °C and enclosed in a membrane of cow gut. After 30 min, the blood meal was removed and a fresh one was introduced [43].

Acute Toxicity on *Anopheles stephensi*

Twenty-five *A. stephensi larvae* (I, II, III and IV instar) or pupae were placed for 24 h in a glass beaker filled with 250 mL of dechlorinated water in a 500 mL glass beaker, and 1 mL of the desired concentration of GQD was added and replicated for five times against all instars. Larval food (0.5 mg) was provided for each tested concentration [44]. Control mosquitoes were exposed for 24 h to the corresponding concentration of the solvent. Percentage mortality was calculated as follows:

$$\text{Percentage mortality} = (\text{number of dead individuals}/\text{number of treated individuals}) \times 100$$

In vitro Cultivation of *Plasmodium falciparum*

Following the method by Murugan et al. [35], here a CQ-sensitive strain 3D7 and CQ-resistant strain INDO of *P. falciparum* were used in in vitro blood stage culture to test the anti-malarial efficacy of GQDs. The culture was carried out at G. Kuppusamy Naidu Memorial Hospital (Coimbatore, India). *P. falciparum* culture was maintained according to the method described by Trager and Jensen [46], with minor modifications. *P. falciparum* (3D7) cultures were maintained in fresh O^{+ve} human erythrocytes suspended at 4 % hematocrit in RPMI 1640, containing 0.2 % sodium bicarbonate, 0.5 % albumax, 45 μg/L hypoxanthine and 50 μg/L gentamycin and incubated at 37 °C under a gas mixture of 5 % O_2, 5 % CO_2 and 90 % N_2. Every day, infected erythrocytes were transferred into a fresh complete medium to propagate the culture. For *P. falciparum* (INDO strain) in culture medium, albumax was replaced by 10 % pooled human serum.

In vitro Antiplasmodial Activity

Control stock solutions of CQ were prepared in water (milli-Q grade); the tested GQDs were prepared in dimethyl sulfoxide (DMSO). All stocks were diluted with culture medium to achieve the required concentrations (in all cases except CQ, the final solution contained 0.4 % DMSO, which was found to be non-toxic to the parasite). Then, GQDs were placed in 96-well flat-bottom tissue culture-grade plates.

GQDs were evaluated for anti-malarial activity against *P. falciparum* strains 3D7 and INDO. For drug screening, SYBR green I-based fluorescence assay was used following the method by Smilkstein et al. [47]. Sorbitol-synchronized parasites were incubated under normal culture conditions at 2 % hematocrit and 1 % parasitemia in the absence or presence of increasing concentrations of samples, where CQ was used as positive control. After 48 h of incubation, 100 μL of SYBR Green I solution {0.2 μL of 10000 X SYBR Green I (In vitrogen)/mL} in lysis buffer [Tris (20 mM; pH 7.5), EDTA (5 mM), saponin (0.008 %; w/v) and Triton X-100 (0.08 %; v/v)] was added to each well and mixed gently twice with a multi-channel pipette and incubated in the dark at 37 °C for 1 h. Fluorescence was measured with a Victor fluorescence multi-well plate reader (Perkin Elmer) with excitation and emission wavelength bands centered at 485 and 530 nm, respectively. The fluorescence counts were plotted against the drug concentration and the 50 % inhibitory concentration (IC_{50}) was determined by an analysis of dose–response curves. Results were validated microscopically by the examination of Giemsa-stained smears of extract-treated parasite cultures [48, 35].

In vivo Antiplasmodial Activity

Following the method by Rajakumar et al. [49] and Murugan et al. [50], male albino mice (weight: 27–30 g) were tested; the animal were fed ad libitum with standard mouse cubes (Barastoc) and clean drinking water. Animals were sexed and caged in groups of five. The animals were housed in the Animal House in Kovai Medical

Centre and Hospital, College of Pharmacy, Coimbatore. Experiments were performed following the Peters' 4-day curative standard test [51–53]. For each bioassay, three albino mice were used to test the antimalarial potential of GQDs. Chloroquine-treated (Sigma-Aldrich) and untreated control groups of mice were tested separately as positive and negative controls [50]. The GQDs were orally administered to the test groups of mice infected by *Plasmodium berghei* at different dose levels, from 0 to 4 days. Chloroquine was used as a standard drug with normal saline (0.9 %) at 5 (mg/kg) was used as positive and the negative control group received distilled water (1 mL).

Parasitemia was monitored in all the groups starting from 0 to 4 days using thin smears of blood films made from the tail vein of the mice [54]. After incubation for 24 h, Giemsa-stained thin blood films were prepared for each mice, and the percentage of inhibition of parasite growth was determined under a microscope. The percent inhibition at each concentration was determined. The percentage of chemosuppression of the total parasitemia for each dose was calculated as:[(A−B/A] × 100 as described by Argotte et al. [55], where A is the mean parasitemia in the untreated control group and B is the parasitemia in each experimental group. Animals from the treated and control groups were followed up until the end of the experiment (10 days after being infected), and the blood samples were taken from all the experimental animals to estimate parasitemia [50].

Impact on Non-target Mosquito Predators

Here, the predation efficiency of mosquitofish *G. affinis*, dragonfly nymph *A. immaculifrons*, Indian bullfrog *H. tigerinus* was assessed against *A. stephensi* larvae. Following the method by Murugan et al. [56], for each instar, 200 mosquitoes were introduced, with an adult fish, a dragonfly nymph or a tadpole in a 500-mL glass beaker containing 250 mL of dechlorinated water. Mosquito larvae were replaced daily with new ones. For each mosquito instar, five replicates were conducted. Control was 250 mL of dechlorinated water without predators. All beakers were checked after 12 and 24 h, and the number of missing preys, assumed as eaten by the predator, was recorded. Missing mosquito larvae were replaced after each daily check with new ones. Predation efficiency was calculated using the following formula:

$$\text{Predatory efficiency} = \frac{(\text{number of consumed mosquitoes}/\text{number of predators})}{\text{total number of mosquitoes}} \times 100.$$

Furthermore, the predation efficiency of *G. affinis*, dragonfly nymphs *A. immaculifrons* and Indian bullfrogs *H. tigerinus* was also evaluated post-treatment with ultra-low doses of GQDs. For each instar, 200 mosquitoes were introduced with 1 fish, 1 dragonfly nymph or 1 tadpole in a 500-mL glass beaker filled with 250 mL of dechlorinated water plus the desired concentration of GQDs (i.e. 1/3 of the LC_{50} calculated against the tested larval instar of *A. stephensi,* [57]. Mosquito larvae were replaced daily with new ones. For each mosquito instar, five replicates

were conducted. Control was dechlorinated water without predators. All beakers were checked after 12 and 24 h and the number of prey consumed by each predator species was recorded. Then, the predation efficiency of each mosquito natural enemy was calculated using the above-mentioned formula.

Data Analysis

SPSS software package 16.0 version was used for all analyses. Data from larvicidal and pupicidal experiments were analyzed by probit analysis, calculating LC_{50} and LC_{90} [58]. Similarly, concerning in vitro antiplasmodial assays, the GQDs and chloroquine concentrations causing 50 % inhibition of parasite growth (IC_{50}) were calculated from the drug concentration–response curves. As regard to in vivo antiplasmodial assays, all values are expressed as percentage growth inhibition. Inhibition data were transformed into arcsine$\sqrt{\text{proportion}}$ values, and analyzed using ANOVA with two factors (i.e. tested drug and dose). Means were separated using Tukey's HSD test ($P < 0.05$).

Results and Discussion

Characterization of Graphene Quantum Dots

GQD were synthesized following the modified method by Hummers where an orange yellow solution was obtained in photo-Fenton reaction of graphene oxide [59]. Graphene with 50 wt% $KMnO_4$ was successfully sheared as tiny dots by acidic suspension and the excess of $KMnO_4$ was consumed by hydrothermal process. Finally, a deep yellow solution dialyzed to get the final product of greenish fluorescent GQDs was freeze-dried and used for further assays. The synthetic process is cheap and relatively simple without the help of strong acid to cut large graphene oxide. Furthemore, the synthesis was in aqueous solution and the product yield is about 34.8 % in weight, higher than the other reported GQD synthesis routes [8, 60].

The purified GQDs were characterized using biophysical techniques including UV–vis, photoluminescence, FTIR and Raman spectroscopy, XRD analysis and TEM, which confirmed the effective nanosynthesis of GQDs (Fig. 1). UV–vis and PL spectra of the nanosynthesized GQDs were shown in Fig. 1a and b. The UV–vis spectrum showed two sharp peaks at 285 and 325 nm by emits bright green fluorescence when irradiated by a UV light, which was assigned to π–π^* absorption peak at 285 nm, a new absorption band at 325 nm was similar with the results by Fan et al. [61]. The UV spectrum of graphene is also affected on reduction, wherein the intensity of the maximum band decreases progressively, with a new long tail band appeared at higher wavelength [62]. Similarly, the PL spectrum (Fig. 1b) exhibited a peak at 505 nm. This excitation-independent PL behavior is different from most of the reported carbon-based nanomaterials [63, 64], which were dependent on excitation wavelength and always shifted to longer wavelengths. This

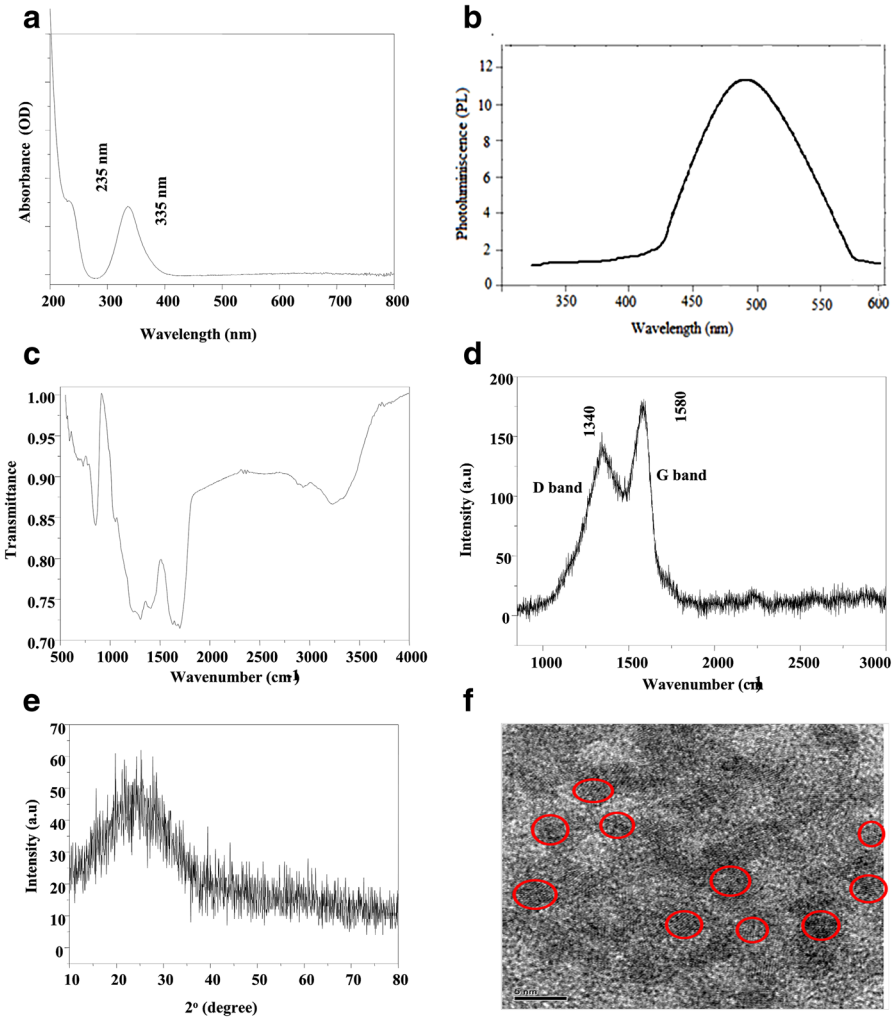

Fig. 1 Biophysical characterization of nanofabricated graphene quantum dots: **a** UV–visible spectrum; **b** photoluminescence (PL) spectrum at 505 nm; **c** functional group prediction by FTIR spectroscopy; **d** Raman spectrum; **e** XRD analysis; **f** TEM

special feature may result from less surface defects and more uniform size of GQDs [65].

The GQDs synthesized here were characterized for their functional groups by FTIR spectroscopy, as reported by Fig. 1c. The carboxyl and hydroxyl groups were absorbed, where the stretching vibrations of OH was intense showing a broad band at 3235-OH cm^{-1} and carboxylic acid stretching vibration ranged at 1200–1400 cm^{-1}. The stretching vibration at 1688 cm^{-1} may be due to C=C. The presence of aromatic groups from proteins and peptides was confirmed by the presence of carbonyl (C=O) stretching vibration at 1613 cm^{-1} from the amide

functional groups [10]. 850 cm^{-1} probably correspond to out of plane C–H vibration. These FTIR spectrum at various stretching vibration showed that the dispersion of GQDs nanocomposite into aqueous medium was in accordance with Wang et al. [66].

The effective synthesis of GQDs was confirmed by Raman spectrum (Fig. 1d). Intense Raman D bands were observed at 1340 cm^1 and G band at 1580 cm^1. These bands are similar to those reported for high quality few-layer graphene nanoribbons [67]. The unique small ratio indicates fewer defects of the GQDs developed by chemical oxidation and exfoliation method over those synthesized by other methods [68]. The XRD pattern of GQDs represented in Fig. 1e predicted the board peak at diffraction plane (002), centered at around 24.12; the interlayer d spacing was found to be 0.36 nm, which is broader than that of graphite [69]. TEM of GQDs was reported in Fig. 1f, showing evenly distributed uniform size of tiny GQDs at 4–5 nm, in good agreement to the 5 nm-GQDs synthesized by cutting graphene oxide sheets as reported using the Hummers method slightly modified by Fan et al. [61].

Cytotoxicity of Graphene Quantum Dots on Breast Cancer Cells

The MTT assay was performed to assess the in vitro cytotoxicity of GQDs against human breast carcinoma (MCF-7) cell lines. GQDs exerted cytotoxicity on MCF-7 cells in a dose-dependent manner (Fig. 2a). The IC_{50} value of GQDs was 24.81 μg/mL after 48 h from the treatment. Nanosynthesized GQDs could be quickly internalized into the cells interacting with the functional groups of intracellular proteins as well as with the nitrogen bases and phosphate groups in DNA. This interaction helps GQDs to decrease the cell viability by alterations in the nuclear morphology, cytoplasm organization, and changes in gene expression of MCF-7 cells. Nitrogen-doped GQDs were co-cultured with HeLa cells and did not showed considerable toxicity on HeLa cells by 3-(4, 5-dimeth-ylthiazol-2-yl)-2, 5-diphenyl tetrazolium bromide test (MTT) assay [60], see also [70]. To our mind, GQDs are a possible candidate to inhibit tumor progression and thereby effectively controlling the disease progression without toxicity towards normal cells.

Apoptosis is an important regulatory pathway of cell growth and proliferation in which cells respond to specific induction signals by initiating intracellular processes that result in characteristic physiological changes occurring over few hours [71]. Using flow cytometry at 488 nm, the apoptotic cells were separated from normal cells, exploiting their reduced DNA content. The induction of apoptosis was higher in GQDs-treated cells post-exposure to the doses of 1.88, 3.75, 7.5, 1.5 and 30 μg/mL. In agreement with Jaganathan et al. [42], the apoptotic percentage of MCF-7 cells increased significantly ($P < 0.001$) with the GQD tested dose (i.e. from 1.9 to 8.4 %) (Fig. 2b). Results suggested that GQDs are able to trigger Bax/Bcl-2/cytochrome c/caspase-3 signaling pathway, activating apoptosis of MCF-7 cells (see also [42]).

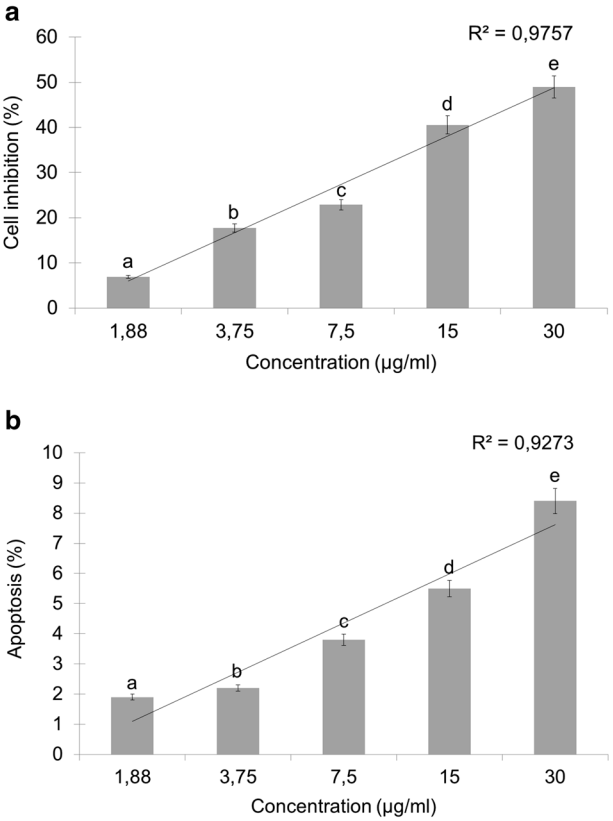

Fig. 2 Toxicity of graphene quantum dots against MCF-7 cancer cell lines: **a** cell growth inhibition (%); **b** graphene quantum dots-triggered cell apoptosis, monitored using flow cytometry at 488 nm. Above each column, *different letters* indicate significant differences among treatments (ANOVA, Tukey's HSD test, $P < 0.05$)

Hemolytic Activity

The extent of hemolysis in malaria is greater if compared to other parasites inducing hemolytic states. Here in vitro blood companionable of GQDs was assessed as hemolytic activity from the whole blood of healthy adult volunteers. The absorbance spectrum of the supernatant of RBC suspension 0.5 % (v/v) incubated with Triton X-100 1 % (v/v) and negative control tyrode was measured at wavelength of 550 nm and the percentage of hemolytic was given in Fig. 3. It was noted that GQDs should be tested at rather high doses (i.e. 1, 5, 10, 15, 20 and 25 µg) to induce hemolytic activity (i.e. 3.26, 10.7, 40, 60.92 and 80.95 %, respecitvely). This activity may be due the action of GQDs on the RBC membrane, if compared to the positive control (1 % Triton X-100) and negative control (tyrode). The binding of GQDs to the RBC molecule can be linked to the small particle size of GQDs which is also linked to the strong electrostatic interactions with phosphatidylcholine lipids present on the surface of the RBC membrane [72].

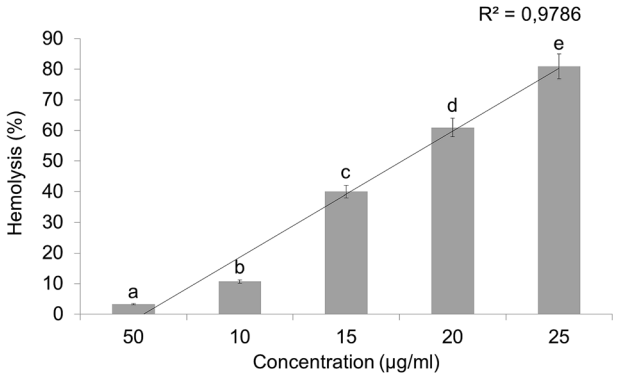

Fig. 3 Hemolysis induced in red blood cells incubated with different concentrations of graphene quantum dots. Above each column, *different letters* indicate significant differences among treatments (ANOVA, Tukey's HSD test, $P < 0.05$)

In agreement with our findings, the size-dependent cytotoxicity on human RBCs and mammalian cells has been reported earlier testing other nanoparticles, such as silica [73, 74] and latex ones [75]. In addition, studies on hemolytic activity of silver nanoparticles showed that the release of low silver ion concentrations leads to the death of RBC molecule [76]. In this scenario, from our results of hemolytic activity assays, we believe that GQDs could represent a better candidate in preventing the destruction of RBC membrane induced by malarial parasites, if compared to metal nanoparticles.

Mosquitocidal and Antiplasmodial Potential

GQDs were toxic against larvae and pupae of the malaria vector *A. stephensi*. LC_{50} values were 0.157 (larva I), 2.756 ppm (II), 3.055 ppm (III), 4.884 ppm (IV) and 6.323 ppm (pupa) (Table 1) respectively. In latest years, a growing number of nanocomposites have been studied for their toxic activity against young instars of several mosquito vectors (e.g. [11, 25, 36, 37, 44, 45, 77–80]). A good example is the larvicidal activity of *Sargassum muticum*-synthesized Ag nanoparticles against larval instars and pupae of *A. aegypti, A. stephensi,* and *C. quinquefasciatus* [81]. Recently, Subramaniam et al. [82] highlighted that low doses of Au nanoparticles synthesized using flower extract of *Corocoupita guianensis* are highly toxic to *A. stephensi* larvae and pupae, with LC_{50} of 17.36 ppm (I), 19.79 ppm (II), 21.69 ppm (III), 24.57 ppm (IV), and 28.78 ppm (pupae), respectively. However, despite these interesting evidences, limited efforts are still available on the precise mechanism(s) of action of nanoparticles against mosquitoes [25].

In the in vitro antiplasmodial assays, GQDs showed high activity against *P. falciparum* if compared to CQ. Indeed, GQDs IC_{50} were 82.43 µg/mL (CQ-s) and 85.17 µg/mL (CQ-r), while IC_{50} of CQ were 90 µg/mL (CQ-s) and 95 µg/mL (CQ-r) (Fig. 4). In agreement with these results, Murugan et al. [35] recently pointed out the high antiplasmodial activity of Ag nanoparticles fabricated using a non-toxic and cheap aqueous extract of the seaweed *Ulva lactuca* on *P. falciparum.* IC_{50} were

Table 1 Acute toxicity of nanofabricated graphene quantum dots on young instars of the malaria vector *Anopheles stephensi*

Target	LC_{50} (LC_{90})	95 % Confidence limit LC_{50} (LC_{90})		Regression equation	χ^2 (*d.f.* = 4)
		Lower	Upper		
Larva I	0.157 (7.361)	0.157 (6.599)	2.35 (8.460)	$y = 0.322 + 0.218x$	5.11 n.s
Larva II	2.756 (8.508)	1.831 (7.704)	3.437 (9.660)	$y = 0.614 + 0.223x$	2.512 n.s
Larva III	3.055 (10.593)	1.763 (8.971)	3.875(13.773)	$y = 0.519 + 0.170x$	0.736 n.s
Larva IV	4.884 (13.520)	3.952 (11.716)	5.653 (16.615)	$y = 0.725 + 0.148x$	0.975 n.s
Pupa	6.323 (13.994)	5.643 (12.293)	7.064 (16.748)	$y = 1.060 + 0.167x$	0.807 n.s

No mortality was observed in the control

LC_{50} lethal concentration that kills 50 % of the exposed organisms

LC_{90} lethal concentration that kills 90 % of the exposed organisms

χ^2 Chi square value

d.f. degrees of freedom

n.s. not significant ($\alpha = 0.05$)

76.33 µg/mL (CQ-s) and 79.13 µg/mL (CQ-r). In addition, Murugan et al. [50] also showed that even neem seed kernel-synthesized Ag nanoparticles achieved comparable IC_{50} on *P. falciparum*, i.e. 82.41 µg/mL (CQ-s) and 86.12 µg/mL (CQ-r). As recently summarized by Benelli [25], the antiplasmodial effectiveness of the above-mentioned nano formulations may due the inhibition of *Plasmodium* merozoite invasion into erythrocytes. However, further studies on these potential mechanisms are needed.

In vivo antiplasmodial experiments highlighted that, after being inoculated intraperitoneally with 1×10^7 *P. berghei* infected RBCs, the untreated control showed progressively increasing parasitemia. Peters' 4-day chemo suppressive activity tests conducted with GQDs showed dose-dependent chemo suppression

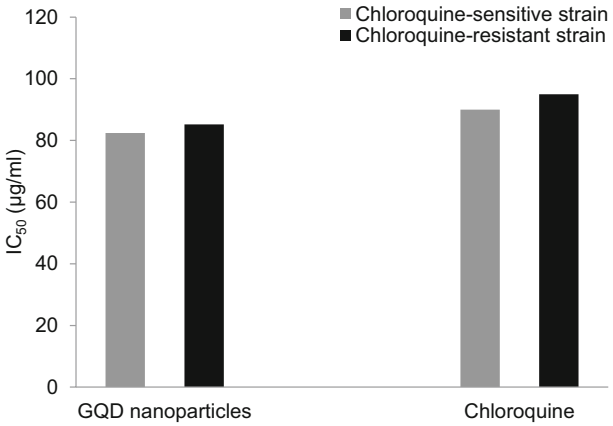

Fig. 4 In vitro growth inhibition of chloroquine-sensitive and chloroquine-resistant strains of *P. falciparum* post-treatment with graphene quantum dots (GQD) and chloroquine

Table 2 In vivo growth inhibition of *Plasmodium berghei* parasites infecting albino mice post-treatment with graphene quantum dots or chloroquine

Treatment	Dose (mg/kg/day)	Suppression of parasitemia at day 4 (%)	Chemosuppression (%)
Graphene quantum dots	5	58.9 ± 0.6	6.72 ± 0.38^{b}
	10	52.8 ± 0.21	8.6 ± 1.01^{bc}
	15	45.4 ± 1.02	9.4 ± 1.02^{cd}
	20	26.4 ± 0.8	15.6 ± 1.2^{d}
	25	23.6 ± 1.01	26.6 ± 0.49^{e}
	30	14.8 ± 1.33	28.6 ± 0.49^{f}
Chloroquine	5	1.0 ± 0.00	100 ± 0.00^{g}
Distilled water	–	53.78 ± 0.2	0.00 ± 0.00^{a}

(Table 2). After four days from the treatment with GQDs, the mean parasitemia (%) of the test groups ranged from 14.8 ± 1.33 to 58.9 ± 0.6 respectively (Table 2). Similarly, Rajakumar et al. [49] showed that dose-dependent suppression of parasitemia triggered by *Eclipta prostrata*-synthesized palladium nanoparticles on *P. berghei* in Swiss albino mice. In our assays, the highest suppression of parasitemia was observed at the dose of 30 mg/kg/day in albino mice, while only 5 mg/kg/day of CQ were needed to completely suppress *P. berghei*. In agreement with Murugan et al. [50], this pointed out the crucial importance of in vivo tests, which should always follow in vitro screenings, since in vivo effectiveness often differs from promising in vitro results. To the best of our knowledge, this is the first in in vivo evaluation of the effectiveness of GQDs on malaria parasites.

Impact on Non-Target Mosquito Predators

Here, we studied the impact of GQDs on the predation activity of adults of the mosquito fish *G. affinis,* nymphs of the dragonfly *A. immaculifrons*, and tadpoles of the Indian bullfrogs *H. tigerinus* against *Anopheles stephensi* young instars. In standard laboratory conditions, *G. affins, A. immaculifrons*, and *H. tigerinus* actively predated on *A. stephensi* (Table 3). Predation efficiency towards *A. stephensi* was 68.2 % (larva II) 58.35 % (larva III) for *G. affinis,* 53.9 % (larva II) and 48.65 % (larva III) for *A. immaculifrons,* and 53 % (larva II) and 41.35 % (larva III) for *H. tigerinus.* In agreement with our data, *G. affinis* has been recently reported as a more efficient predator of mosquito young instars if compared to other aquatic organisms, such as Belostomatidae and odonate nymphs [83]. However, Bowatte et al. [84] also highlighted the role of *Bufo, Euphlyctis, Hoplobatrachus, Polypedates*, and *Ramanella* tadpoles in reducing mosquito populations through predation on mosquito eggs.

Notably, post-treatment with GQDs, the predation efficiency were boosted to 96.5 % (larva II) and 88.8 % (larva III) for *G. affinis,* 88.1 % (larva II) and 81.6 % (larva III) for *A. immaculifrons,* and 84.1 % (larva II) and 75.15 % (larva III) for *H. tigerinus*, respectively (Table 3). To the best of our knowledge, scarce information

Table 3 Impact of nanofabricated graphene quantum dots (GQD) on the predation efficiency of three natural enemies of *Anopheles stephensi* young instars: the adults of larvivorous fish *Gambusia affinis,* the nymphs of dragonfly *Anax immaculifrons*, and the tadpoles of Asian bullfrog *Hoplobatrachus tigerinus*

Predator species	Treatment	Target	Predation (%)		Mean predation (%)
			Daylight time	Night time	
G. affinis	Standard conditions	Larva II	72.0 ± 1.0^{e}	64.5 ± 1.2^{d}	68.2^{d}
		Larva III	60.6 ± 0.8^{f}	56.1 ± 1.1^{e}	58.35^{e}
	Post-treatment with GQD[§]	Larva II	97.5 ± 1.1^{a}	95.8 ± 1.1^{a}	96.5^{a}
		Larva III	91.1 ± 1.0^{b}	86.5 ± 1.3^{b}	88.8^{b}
A. immaculifrons	Standard conditions	Larva II	56.3 ± 1.5^{f}	51.5 ± 1.3^{ef}	53.9^{e}
		Larva III	50.1 ± 0.7^{g}	47.2 ± 1.2^{f}	48.65^{f}
	Post-treatment with GQD[§]	Larva II	90.2 ± 0.7^{b}	86.0 ± 0.7^{b}	88.1^{b}
		Larva III	83.0 ± 1.7^{c}	80.2 ± 0.7^{bc}	81.6^{bc}
H. tigerinus	Standard conditions	Larva II	56.9 ± 2.1^{f}	49.1 ± 1.0^{f}	53.0^{e}
		Larva III	42.6 ± 1.6^{h}	40.1 ± 1.1^{g}	41.35^{g}
	Post-treatment with GQD[§]	Larva II	87.9 ± 1.7^{bc}	80.3 ± 1.2^{bc}	84.1^{b}
		Larva III	78.4 ± 1.6^{d}	71.9 ± 1.6^{c}	75.15^{c}

[§] see text for the tested dosage

Predation rates are mean ± SD of five replicates (1 predator vs. 200 *A. stephensi* larvae per replicate)

Control was clean water, without mosquito predators

Within each column, values followed by different letter(s) are significantly different (generalized linear model, $P < 0.05$)

is available about how ultra-low dosages of nanoparticles impact behavioral traits of aquatic organisms sharing the same ecological niche as mosquitoes [11, 25, 32–34, 36, 37, 82]. For instance, Subramaniam et al. [85] reported that *Mimusops elengi*-synthesized silver nanoparticles did not negatively impact predation rates of the mosquitofish *G. affinis* against *A. stephensi* and *Aedes albopictus*, validating this novel control tool in an environment-friendly perspective. As regards to carbon nanoparticles, Murugan et al. [10] have pointed out that a single treatment with 2 ppm of carbon nanoparticles enhanced the predation efficiency of *Lethocerus indicus* against *Culex quinquefasciatus* larvae. As regards to genotoxicity, it has been showed that *Carassius auratus* erythrocytes showed no significant damages at carbon nanoparticle doses lower than 25 ppm [10].

Conclusions

Nowadays, the eco-friendly control of mosquitoes is a key challenge [86]. In this research we focused on the effectiveness of GQDs against *P. falciparum, P. berghei* and young instars of malaria mosquitoes. Notably, the predation efficiency of mosquito natural enemies *G. affinis*, *A. immaculifrons* and *H. tigerinus* post-treatment with an ultra-low dose of GQDs was boosted. In addition, GQDs were

toxic against MCF-7 cancer cell lines with an $IC_{50} = 24.81$ μg/mL and triggered apoptosis in 1.9–8.4 % of treated cells. Overall, this study highlighted the concrete potential of GQDs for the development of newer and safer drugs in the fight against *Anopheles* vectors, *Plasmodium* parasites and breast cancer cells. Extensive field assays based on the employ of GQDs against mosquito vectors are urgently required.

Acknowledgments Three anonymous reviewers improved an earlier version of this work. Dr. Anitha Jaganathan is grateful to the University Grant Commission (New Delhi, India), Project No. PDFSS-2014-15-SC-TAM-10125. Dr. Devakumar Dinesh would like to extend his sincere thanks for UGC (New Delhi, India) for granting RGNF-2015-17-SC-TAM-27906.

Compliance with ethical standards

Conflicts of Interest The Authors declare no competing interests.

References

1. N. Li, A. Than, X. Wang, S. Xu, L. Sun, H. Duan, C. Xu, and P. Chen (2016). *ACS. Nano.* **10**, (3), 3622–3629. doi:10.1021/acsnano5b08103.
2. S. N. Baker and G. A. Baker (2010). *Angew. Chemie.* **49**, (38), 6726–6744.
3. J. C. G. EstevesdaSilva and H. M. R. Goncalves (2011). *Trends. Analyt. Chem.* **30**, (8), 1327–1336.
4. J. Shen, Y. Zhu, X. Yang, and C. Li (2012). *Chem. Comm.* **48**, (31), 3686–3699.
5. W. H. De Jong and P. J. A. Borm (2008). *Int. J. Nanomed.* **3**, (2), 133–149.
6. W. C. Lee, C. Haley, Y. X. Lim, H. Shi, A. Lena, L. Tang, Y. Wang, C. T. Lim, and K. P. Loh (2011). *ACS. Nano.* **5**, (9), 7334–7341.
7. X. C. Yuan, Z. M. Liu, Z. Y. Guo, Y. H. Ji, M. Jin, and X. P. Wang (2014). *Nanoscale. Res. Lett* **9**, 108.
8. D. Jiang, Y. Chen, N. Li, W. Li, Z. Wang, Jingli Zhu, H. Zhang, B. Liu, and S. Xu (2015). *PLOS ONE* **10**, (12), e0144906.
9. M. Saxena, Sumit Kumar Sonkarb, and Sabyasachi Sarkar (2013). *RSC. Adv.* **3**, 22504–22508.
10. K. Murugan, D. Nataraj, P. Madhiyazhagan, V. Sujitha, B. Chandramohan, C. Panneerselvam, D. Dinesh, R. Chandirasekar, K. Kovendan, U. Suresh, J. Subramaniam, M. Paulpandi, C. Vadivalagan, R. Rajaganesh, H. Wei, B. Syuhei, A. T. Aziz, M. Saleh Alsalhi, S. Devanesan, M. Nicoletti, A. Canale, and G. Benelli (2016). *Parasitol. Res.* **115**, 1071–1083.
11. G. Benelli (2016). *Parasitol. Res.* **115**, 23–34.
12. L. M. Rueda (2008). *Dev Hydrobiol* **595**, (1), 477–487.
13. G. Benelli (2015). *Parasitol. Res.* **114**, 2801–2805.
14. Mehlhorn H (ed) (2015) Encyclopedia of parasitology, 4th edn. Springer, New 893, York
15. G. Benelli (2016). *Asia. Pacif. J. Trop. Biomed.* **6**, 353–354.
16. G. Benelli, A. Canale, A. Higuchi, K. Murugan, R. Pavela, and M. Nicoletti (2016). *Asia. Pacif. J. Trop. Dis.* **6**, 253–258.
17. WHO (2016) Malaria Fact sheet, Updated January 2016
18. J. M. Cohen, D. L. Smith, C. Cotter, A. Ward, and G. Yamey (2012). *Malaria. J.* **11**, 122.
19. G. Benelli and H. Mehlhorn (2016). *Parasitol. Res.* **115**, 1747–1754.
20. V. Sharma, Rohini Samant, Ashit Hegde, and Khushrav Bhaja (2012). *JAPI* **60**, 51–55.
21. G. Dhaliwal, P. A. Cornett, and L. M. Tierney (1979). *Am. Fam. Physician.* **69**, 2599–2606.
22. S. Lehrer (2010). *Med. Hypotheses.* **74**, 167–168.
23. S. Lehrer (2010). *Anticancer. Res.* **30**, 1371–1373.
24. G. Benelli, A. Lo Iacono, A. Canale, and H. Mehlhorn (2016). *Parasitol. Res.* **115**, 2131–2137.
25. G. Benelli (2016). *Enzyme. Microbial. Technol.*. doi:10.1016/j.enzmictec.2016.08.022.
26. A. F. Howard, G. Zhou, and F. X. Omlin (2007). *BMC. Public. Health.* **7**, 199.
27. J. Hemingway and H. Ranson (2000). *Annu. Rev. Entomol.* **45**, 371–391.

28. K. Raghvendra (2002). *ICMR Bull* **32**, (10), 1–7.
29. M. N. Naqqash, A. Gökçe, A. Bakhsh, and M. Salim (2016). *Parasitol. Res.* **115**, 1363–1373.
30. C. D. Linde *Physicochemical properties and environment fate of pesticides* (Environmental Hazards Assessment Program, California, 1994). **9**.
31. Lini K. Mathew (2016). *Int. J. Adv Res.* **4**, (3), 1734–1739.
32. K. Murugan, D. Dinesh, M. Paulpandi, A. D. Althbyani, J. Subramaniam, P. Madhiyazhagan, L. Wang, U. Suresh, P. M. Kumar, J. Mohan, R. Rajaganesh, H. Wei, K. Kalimuthu, M. N. Parajulee, H. Mehlhorn, and G. Benelli (2015). *Parasitol. Res.* **114**, 4349–4361.
33. K. Murugan, G. Benelli, C. Panneerselvam, J. Subramaniam, T. Jeyalalitha, D. Dinesh, M. Nicoletti, J. S. Hwang, U. Suresh, and P. Madhiyazhagan (2015). *Exp. Parasitol.* **153**, 129–138.
34. K. Murugan, V. Priyanka, D. Dinesh, P. Madhiyazhagan, C. Panneerselvam, J. Subramaniam, U. Suresh, B. Chandramohan, M. Roni, M. Nicoletti, A. A. Alarfaj, A. Higuchi, M. A. Munusamy, H. F. Khater, R. H. Messing, and G. Benelli (2015). *Parasitol. Res.* **114**, 3601–3610.
35. K. Murugan, C. M. Samidoss, C. Panneerselvam, A. Higuchi, M. Roni, U. Suresh, B. Chandramohan, J. Subramaniam, P. Madhiyazhagan, D. Dinesh, R. Rajaganesh, A. A. Alarfaj, M. Nicoletti, S. Kumar, H. Wei, A. Canale, H. Mehlhorn, and G. Benelli (2015). *Parasitol. Res.* **114**, 4087–4097.
36. M. Govindarajan and G. Benelli (2016). *Parasitol. Res.*. doi:10.1007/s00436-015-4817-0.
37. M. Govindarajan and G. Benelli (2016). *RSC Adv* **6**, 59021–59029.
38. W. S. Hummers and R. E. Offeman (1958). *J. Am. Chem. Soc* **80**, 1339.
39. T. Mosmann (1983). *J. Immunol. Methods.* **65**, 55–63.
40. K. Murugan, D. Dinesh, K. Kavithaa, M. Paulpandi, T. Ponraj, M. Saleh Alsalhi, S. Devanesan, J. Subramaniam, R. Rajaganesh, H. Wei, K. Suresh, M. Nicoletti, and G. Benelli (2016). *Parasitol. Res.* **115**, 1085–1096.
41. A. Monks, D. Scudiero, P. Skehan, R. Shoemaker, K. Paull, D. Vistica, C. Hose, J. Langley, P. Cronise, A. Vaigro-Wolff, M. Gray-Goodrich, et al. (1991). *J. Natl. Cancer. Inst.* **83**, 757–766.
42. A. Jaganathan, K. Murugan, C. Panneerselvam, P. Madhiyazhagan, D. Dinesh, C. Vadivalagan, Al Thabiani Aziz, B. Chandramohan, U. Suresh, R. Rajaganesh, J. Subramaniam, M. Nicoletti, A. Higuchi, A. A. Alarfaj, M. A. Munusamy, Suresh Kumar, and G. Benelli (2016). *Parasitol. Int.* **65**, 276–284.
43. K. Murugan, M. Aamina Labeeba, C. Panneerselvam, D. Dinesh, U. Suresh, J. Subramaniam, P. Madhiyazhagan, J. S. Hwang, L. Wang, M. Nicoletti, and G. Benelli (2015). *Res. Vet. Sci.* **102**, 127–135.
44. D. Dinesh, K. Murugan, P. Madhiyazhagan, C. Panneerselvam, M. Nicoletti, W. Jiang, G. Benelli, B. Chandramohan, and U. Suresh (2015). *Parasitol. Res.* **14**, 1519–1529.
45. U. Suresh, K. Murugan, G. Benelli, M. Nicoletti, D. R. Barnard, C. Panneerselvam, P. Mahesh Kumar, J. Subramaniam, D. Dinesh, and B. Chandramohan (2015). *Parasitol. Res.* **114**, 1551–1562.
46. W. Trager and J. Jensen (1976). *Science* **193**, 673–675.
47. M. Smilkstein, N. Sriwilaijaroen, J. X. Kelly, P. Wilairat, and M. Riscoe (2004). *Antimicrob. Agents. Chemother.* **48**, 1803–1806.
48. E. Bensoussan, A. Nasereddin, F. Jonas, L. F. Schnur, and C. L. Jaffe (2006). *J. Clin. Microbiol.* **44**, (4), 1435–1439.
49. G. Rajakumar, A. A. Rahuman, I. M. Chung, A. Vishnu Kirthi, S. Marimuthu, and K. Anbarasan (2015). *Parasitol. Res.* **114**, 1397–1406.
50. K. Murugan, C. Panneerselvam, C. M. Samidoss, P. Madhiyazhagan, U. Suresh, M. Roni, B. Chandramohan, J. Subramaniam, D. Dinesh, R. Rajaganesh, M. Paulpandi, H. Wei, A. T. Aziz, M. Saleh Alsalhi, S. Devanesan, M. Nicoletti, R. Pavela, A. Canale, and G. Benelli (2016). *Res. Vet. Sci.* **106**, 14–22.
51. W. Peters, J. H. Portus, and B. L. Robinson (1975). *Ann. Trop. Med. Parasitol.* **69**, 155–171.
52. L. T. Peter and V. K. Anatoli , *The Current Global Malaria Situation. Malaria: Parasite Biology, Pathogenesis and Protection.* (ASM, Washington, 1998), pp. 11–22
53. A. F. David, J. R. Philip, R. C. Simon, B. Reto, and N. Solomon (2004). *Nat. Rev.* **3**, 509–520.
54. A. C. Ene, S. E. Atawodi, D. A. Ameh, H. O. Kwanshie, and P. U. Agomo (2008). *Trends. Med. Res.* **3**, (1), 16–23.
55. R. R. Argotte, A. G. Ramírez, G. M. C. Rodríguez, et al. (2006). *J. Nat. Prod* **69**, 1442–1444.
56. K. Murugan, C. Panneerselvam, A. T. Aziz, J. Subramaniam, P. Madhiyazhagan, J. S. Hwang, Lan Wang, D. Dinesh, U. Suresh, M. Roni, A. Higuchi, M. Nicoletti, M. Saleh Alsalhi, and G. Benelli (2016). *Environ. Sci. Poll. Res.*. doi:10.1007/s11356-016-6832-9.

57. K. Murugan, J. Anitha, D. Dinesh, U. Suresh, R. Rajaganesh, B. Chandramohan, J. Subramaniam, M. Paulpandi, C. Vadivalagan, P. Amuthavalli, L. Wang, J. S. Hwang, H. Wei, M. S. Alsalhi, S. Devanesan, S. Kumar, K. Pugazhendy, A. Higuchi, M. Nicoletti, and G. Benelli (2016). *Ecotoxicol. Environ. Saf.* **132**, 318–328.
58. D. J. Finney *Probit analysis*, 3rd ed (Cambridge University Press, Cambridge, 1971).
59. X. B. Yan, J. T. Chen, J. Yang, Q. J. Xue, and P. Miele (2010). *ACS. Appl. Mater. Interf.* **2**, (9), 2521–2529.
60. C. Hu, Y. Liu, Y. Yang, J. Cui, Z. Huang, and Y. Wang (2013). *J. Mater. Chem. B.* **1**, 39–42.
61. X. Fan, G. Zhang, and F. Zhang (2015). *Chem. Soc. Rev.* **44**, 3023–3035.
62. C. N. R Rao, U. Maitra and H. S. S. Ramakrishna Matte in C. N. R Rao and A. K. Sood (eds.), *Synthesis, Characterization, and Selected Properties of Graphene* (Wiley, New York, 2013)
63. D. Pan, J. Zhang, Z. Li, and M. Wu (2010). *Adv. Mater.* **22**, 734–738.
64. D. Y. Pan, L. Guo, J. C. Zhang, C. Xi, Q. Xue, and H. Huang (2012). *J. Mater. Chem.* **22**, (8), 3314–3318.
65. S. Zhuo, M. Shao, and S. T. Lee (2012). *ACS. Nano.* **6**, (2), 1059–1064.
66. S. Wang, Z. Chen, I. Cole, and Q. Li (2015). *Carbon* **82**, 304–313.
67. L. Jiao, X. Wang, G. Diankov, H. Hailiang Wang, and H. Dai (2010). *Nat. Nanotechnol.* **5**, (5), 321–325.
68. F. Liu, M. Jang, H. Ha, J. Kim, Y. Cho, and T. Seo (2013). *Adv. Mater.* **25**, 3657–3662.
69. G. Xie, K. Zhang, B. Guo, et al. (2013). *Adv. Mater.* **25**, 3820–3839.
70. H. J. Sun, L. Wu, N. Gao, J. Ren, and X. G. Qu (2013). *ACS. Appl. Mater. Interfaces.* **5**, 1174–1179.
71. A. Z. Mirakabadi, A. Sarzaeem, S. Moradhaseli, A. Sayad, and M. Negahdary (2012). *Iran. J. Cancer. Prev.* **5**, (3), 109–116.
72. K. H. Liao and C. W. Macosko (2011). *ACS. Appl. Mater. Interfaces.* **3**, (7), 2607–2615.
73. Y. S. Lin and C. L. Haynes (2010). *J. Am. Chem. Soc* **132**, 4834–4842.
74. D. Napierska, L. C. J. Thomassen, V. Rabolli, D. Lison, L. Gonzalez, M. Kirsch-Volders, J. A. Martens, and P. H. Hoet (2009). *Small* **5**, 846–853.
75. A. Mayer, M. Vadon, B. Rinner, A. Novak, R. Wintersteiger, and E. Frohlich (2009). *Toxicology* **258**, 139–147.
76. J. Choi, V. Reipa, V. M. Hitchins, P. L. Goering, and R. A. Malinauskas (2011). *Toxicol. Sci.* **123**, 133–143.
77. N. K. Arjunan, K. Murugan, C. Rejeeth, P. Madhiyazhagan, and D. R. Barnard (2012). *Vector. Borne. Zoon. Dis* **12**, (3), 262–268.
78. M. Roni, K. Murugan, C. Panneerselvam, J. Subramaniam, and J. S. Hwang (2013). *Parasitol. Res.* **112**, 981–990.
79. M. Govindarajan, M. Nicoletti, and G. Benelli (2016). *J. Clust. Sci.* **27**, 745–761.
80. M. Govindarajan, S. L. Hoti, M. Rajeswary, and G. Benelli (2016). *Parasitol. Res.*. doi:10.1007/s00436-016-5038-x.
81. P. Madhiyazhagan, K. Murugan, A. Naresh Kumar, T. Nataraj, D. Dinesh, C. Panneerselvam, J. Subramaniam, P. Mahesh Kumar, U. Suresh, M. Roni, M. Nicoletti, A. Abdullah Alarfaj, A. Higuchi, A. Murugan Munusamy, and G. Benelli (2015). *Parasitol. Res.*. doi:10.1007/s00436-015-4671-0.
82. J. Subramaniam, K. Murugan, C. Panneerselvam, K. Kovendan, P. Madhiyazhagan, D. Dinesh, P. Mahesh Kumar, B. Chandramohan, U. Suresh, R. Rajaganesh, Mohamad Saleh Alsalhi, S. Devanesan, M. Nicoletti, A. Canale, and G. Benelli (2016). *Environ. Sci. Pollut. Res.*. doi:10.1007/s11356-015-6007-0.
83. E. Kweka, G. Zhou, T. Gilbreath, Y. Afrane, M. Nyindo, A. Githeko, and G. Yan (2011). *Parasit. Vect.* **4**, 128.
84. G. Bowatte, P. Perera, G. Senevirathne, S. Meegaskumbura, and M. Meegaskumbura (2013). *Biol. Control.* **67**, 469–474.
85. J. Subramaniam, K. Murugan, C. Panneerselvam, K. Kovendan, P. Madhi yazhagan, P. Mahesh Kumar, D. Dinesh, B. Chandramohan, U. Suresh, M. Nicoletti, A. Higuchi, J. S. Hwang, S. Kumar, A. A. Alarfaj, M. A. Munusamy, R. H. Messing, and G. Benelli (2015). *Environ. Sci. Poll. Res.* doi:10.1007/s11356-015-5253-5.
86. G. Benelli (2015). *Parasitol. Res.* **114**, 3201–3212.